Strong-field QED effects induced by high power lasers

Contact Thomas.Heinzl@plymouth.ac.uk

T. Heinzl

University of Plymouth, School of Mathematics and Statistics, Drake Circus, Plymouth, PL4 8AA, UK

Introduction

This contribution presents a brief overview of relativistic laser matter interactions that are best described by *strong-field* quantum electrodynamics (QED). While standard QED is the theory of photons and electrons (and positrons, their antiparticles) *in vacuo* its strong-field generalisation features an additional, strong external field A minimally coupled to the usual QED Hamiltonian. Traditionally A would have represented e.g. the field of a heavy nucleus, but here we focus entirely on fields provided by ultra-intense lasers. The latter have become more and more relevant for extreme-field studies in recent years as technological advances have led to unprecedented magnitudes both in power (> 1 PW) and intensity (> 10^{22} W/cm^2). In this regime of 'extremes' CLF at RAL is in a rather unique position with facilities such as Vulcan (1 PW) and Astra-Gemini (2 × 0.5 PW) and, in particular, the planned upgrade of Vulcan by another order of magnitude in delivered power (10 PW).

At this point it is useful to introduce a dimensionless measure of laser intensity given by the energy gain of an electron (charge e) traversing a laser wave length λ in a field of strength E, measured in units of its rest energy, mc^2,

$$a_0 \equiv eE\lambda/mc^2 \qquad (\lambda = \lambda/2\pi) \tag{1}$$

This definition may be generalized to an explicitly Lorentz and gauge invariant form [1]. In what follows we will assume that the laser is described by a plane wave field, depending solely on the invariant phase,

$$\mathsf{A} = \mathsf{A}(\phi)\,, \quad \phi \equiv \omega_L t - \boldsymbol{k}\cdot\boldsymbol{x}\,, \tag{2}$$

(Lorentz indices suppressed) where ω_L and $\boldsymbol{k}$ denote laser frequency and wave vector, respectively. For such a field one can find an exact solution of the Dirac equation, the so called Volkov electron [2]. From a Feynman diagram point of view this is the basic feature of strong-field QED. Electron lines become dressed ('fat') and now represent Volkov electrons, which may be expanded in terms of ordinary electron lines, see Fig.1.

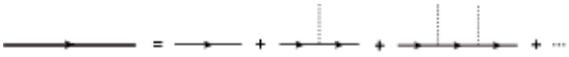

Figure 1. Dressed electron line expressed in terms of bare ones.

The dotted lines in Fig.1 represent the continuous emission and absorption of laser photons, a quantum version of the classical quiver motion of the charge in the field. The dressed electron lines of Fig.1 go along with new Feynman rules which, as usual, translate any Feynman graph one may build from lines and vertices into a formula. For our purposes explicit formulae will not be needed. It is sufficient to keep in mind that all strong-field QED processes can be described in terms of Feynman diagrams which in turn can be translated into S-matrix elements [3]. These are the probability amplitudes for the scattering/decay/emission process in question and finally, by a well defined procedure, lead to cross sections and rates. In what follows we will heavily rely on this intuitive picture.

Vacuum diagrams: spontaneous pair production

The simplest diagrams one can think of are those without external legs. Hence, there are no external particles involved and we are dealing with the vacuum or, more precisely, with transition amplitudes from the past vacuum state into its future pendant. A typical Feynman diagram is given by the vacuum bubble below depicting a Volkov electron loop[1].

Figure 2. Elementary vacuum bubble (Volkov electron loop).

This is the lowest order contribution to the amplitude that the vacuum remains the vacuum (i.e. the 'vacuum persistence amplitude') which may be written as

$$Z[\mathsf{A}] \equiv \langle 0,\mathrm{out}|0,\mathrm{in}\rangle_{\mathsf{A}} = \exp i\left\{ \bigcirc + \ldots \right\} \tag{3}$$

with the ellipses standing for higher orders. For a plane wave all vacuum bubbles turn out to be exactly zero so Z[A] = 1 and the vacuum is stable i.e. remains the

[1] Note that the strong-field Feynman diagrams based on dressed (Volkov) electron lines do not 'resolve' the external laser photons. They can be recovered upon expanding the electron lines as in Fig. 1.

vacuum under the influence of the wave field. This situation changes if we consider different field configurations such as standing waves produced from counter propagating lasers as could be realized with Astra Gemini at CLF. Near the anti-nodes one may even adopt the simple approximation of having a purely electric constant field. In this case the vacuum bubble can be calculated exactly and becomes the celebrated Heisenberg-Euler effective action Γ_{HE}[4]. One finds that this has an imaginary part which is given by the optical theorem (or Kramers-Kronig relation),

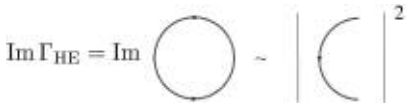

(4)

The right-hand side here (pictorially obtained by 'cutting' the loop and squaring) is the (one-loop) probability of spontaneously producing electron positron pairs from the vacuum with an (approximately) constant field. The total probability is then

$$p = 1 - |Z[\mathsf{A}]|^2 = 1 - e^{-2\mathrm{Im}\,\Gamma_{\mathrm{HE}}} \simeq 2\,\mathrm{Im}\,\Gamma_{\mathrm{HE}} \qquad (5)$$

Working out the imaginary part of the Heisenberg-Euler effective action (or vacuum bubble) one recovers Schwinger's seminal result[5],

$$p \sim E^2\, e^{-\pi E_S/E} \qquad (6)$$

in terms of the ambient electric field E and the QED field strength,

$$E_S \equiv m^2c^3/e\hbar \qquad (7)$$

first obtained by Sauter[6]. Its numerical value is $E_S = 1.3 \times 10^{18}$ V/m corresponding to an intensity $I_S = 4 \times 10^{29}$ W/cm^2. As current or near-future lasers will only reach fields about four orders of magnitude below, the exponential suppression in (6) is enormous. In the actual pair production rate this is somewhat compensated by a pre-exponential factor given by the ratio of the reaction four-volume, determined by focus size and pulse duration, and the Compton four volume. As a result conservative estimates predict that spontaneous pair production may be seen at about 10^{27} W/cm^2 and above [7].

External photons: vacuum polarisation

We have seen that spontaneous pair creation is described in terms of vacuum loops with no external particles being present. If we allow for external (non-laser) photons we gain another parameter, the photon energy ˆ that may be tuned according to our objectives. It is useful to view this as a modification of the vacuum loop of Fig.2 which becomes replaced by the vacuum polarization diagram in (8) representing the polarization tensor (Lorentz indices suppressed).

(8)

Again, this diagram has both a real and an imaginary part and we will discuss them one after the other.

External photons: vacuum birefringence (Re Π)

The real part of the polarisation tensor describes the modifications of the external (probe) photon propagation due to the vacuum polarization loop in the presence of the external field A. Recall that even with external fields being absent the vacuum gets polarized due to the appearance of virtual pairs denoted by the fermion loop. This effect is Lorentz invariant and does not single out preferred directions. Its most important consequence presumably is charge renormalisation due to screening by the polarization cloud of vacuum 'dipoles'. Strong external fields have additional effects which typically are directional. The most important is vacuum birefringence as first discussed in Toll's thesis[8] and recently reviewed by the author and others[9]. In the focus of an intense laser the vacuum develops two different, nontrivial refractive indices given by

$$n_\pm = 1 + \frac{\alpha\epsilon^2}{45\pi}\{11 \pm 3 + \ldots\} \qquad (9)$$

with the ellipses denoting higher order terms in the small parameters $\alpha = 1/137$ (the fine structure constant) and $\varepsilon = E/E_S$ (the reduced electric field). In addition there are corrections depending on the probe frequency, $\nu = \omega/m$, measured in terms of the electron mass. These will become important in a moment. So (9) is the leading order in a weak-field, low-frequency expansion. The indices yield a phase retardation between different polarizations which induces an ellipticity signal when linearly polarized probe photons pass through a laser focus. The ellipticity is found to be[9]

$$\delta^2 = 3.2 \times 10^5 \left(\frac{d}{\mu\mathrm{m}}\epsilon^2\nu\right)^2, \quad \epsilon\nu \ll 1 \qquad (10)$$

To maximize this signal one would like to have frequency, intensity and focus size d as large as possible. For Vulcan (10 PW), for instance, we may assume $\varepsilon = 10^{-3}$, $\nu = 10^{-2}$ (for a hard X-ray source) and $d = 50$ μm. This yields a rather small ellipticity signal $\delta^2 \approx 10^{-7}$, which apparently lies below the current sensitivity of X-ray polarimetry of about 10^{-4} –10^{-5} but may become measurable in the near future.

External photons: induced pair production (Im Π)

As mentioned above, the polarization tensor develops an imaginary part above pair creation threshold. Similarly to (4) it is determined by the optical theorem which now reads

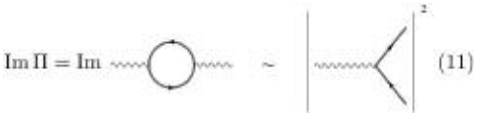

(11)

Again, the right-hand side represents the probability for pair creation but this time it is 'induced' (above threshold) or 'assisted' (below threshold) by the external photon. Expanding the diagram we obtain a sum over all processes $\gamma + n\,\gamma_L \to e^+e^-$. Such a process has actually been observed in the high energy regime in the SLAC E-144 experiment[10] where a 30 GeV γ-beam

was brought into collision with a Terawatt laser. Thus, the threshold was overcome by utilizing the large relativistic gamma factor of about 10^5 boosting the electric field to a supercritical value. The high energy γ's were obtained via Compton backscattering (see below) from the SLAC electron beam. Altogether about 10^2 positrons were observed upon absorption of n=5 laser photons. This is the minimum number required in agreement with an increased production threshold due to the intensity dependent electron mass shift [11]

$$m^2 \to m_*^2 \equiv m^2(1+a_0^2) \qquad (12)$$

SLAC E-144 had a_0 of order unity, so the shift effects should be much more significant at Vulcan (10 PW) where one expects a_0 to be of order 10^2. Clearly, further studies are required here as the calculation of the effective mass (12) is based on infinite plane waves instead of realistic Gaussian beams[2].

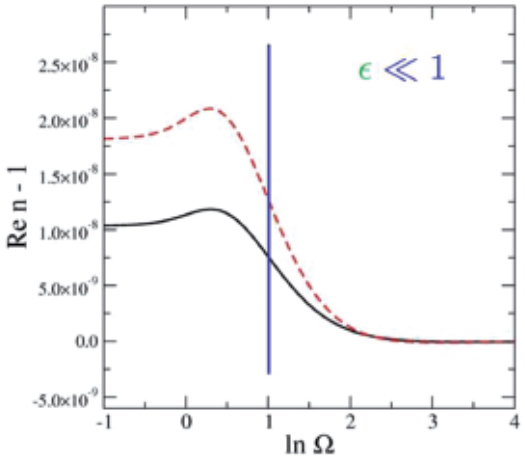

Figure 3. Real part of the refractive indices (9) as a function of ln Ω = ln εv. The negative slope signals anomalous dispersion.

The appearance of an imaginary part is also seen for the refractive indices (9) if one goes to sufficiently large values in the product εv. Following the SLAC example this may be achieved by Compton backscattering of a laser off a high-energy electron beam (of a few GeV, say). These energies can presumably be achieved within the next few years using a mechanism such as laser wake field acceleration (or similar) which has already produced 1 GeV electrons. Real and imaginary parts of the indices are depicted in Figs 3 and 4 as a function of εv (following Toll [8]). The plots are valid for small ε (weak fields) which will be a good approximation for the foreseeable future. The vertical lines mark the parameter values ε$v \approx 3$ which could be obtained, for instance, at Vulcan (10 PW) with γ's backscattered off 10 GeV electrons. In this parameter regime, the real part of the indices develops a negative slope, hence anomalous dispersion.

[2] Analogous remarks apply to spontaneous (vacuum) pair creation.

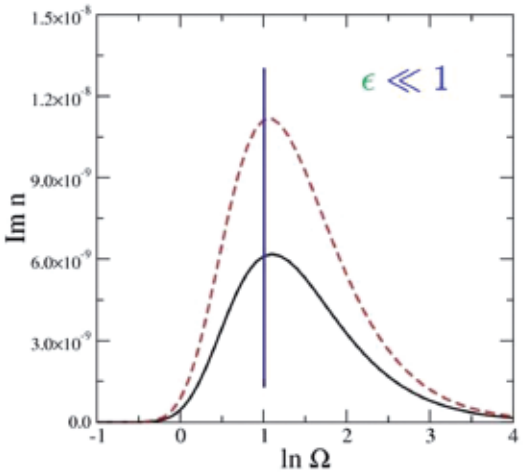

Figure 4. Imaginary part of the refractive indices (9) signaling absorption.

The Kramers-Kronig relations then state that this is a signal of absorption, i.e. a nonvanishing imaginary part and, indeed, this is what one can see in Fig.4. Thus, a careful study of the frequency dependence of the strong-field QED refractive indices can provide an alternative signal for induced pair production.

External electrons: nonlinear Compton scattering

All processes discussed so far had a somewhat unfortunate feature in common: for current and near-future lasers the signals to be expected are quite small. This is due to threshold effects leading to exponential or power law suppression. The appearance of thresholds may be traced to the fact that the previous processes where intrinsically quantum in nature which is particularly obvious for one-loop diagrams as they are known to be of order $\hbar$. Things change, however, if we turn our attention to processes with incoming electrons. The most important of these is obtained from the right-hand side in (11), representing induced pair creation, via crossing symmetry which yields the Feynman diagram for nonlinear Compton scattering as shown in Fig.5.

Figure 5. Feynman diagram for nonlinear Compton scattering (right) obtained from pair production (left) via crossing.

The process in question is the collision of an electron and a high intensity laser beam such that a photon γ is scattered out of the beam. In terms of dressed electrons this is depicted on the right-hand side of Fig.5 which, when expanded in the number of laser photons involved, becomes a superposition of processes of the form $e + n\gamma_L \to e' + \gamma'$ where an electron absorbs an arbitrary number n of laser photons γ_L of energy $\hbar\omega_L \sim 1$ eV before emitting a single photon γ'. Note that the Compton diagram has

a classical limit which is a fair representation of the process when the electron mass m is the dominant energy scale. This classical limit is referred to as Thomson scattering. We re-emphasise that nonlinear Compton/Thomson scattering is not suppressed by any threshold effects. Thus, one can study intensity effects at arbitrarily low centre-of-mass energies both for photons and electrons. This is quite a unique feature of nonlinear Compton/Thomson scattering and singles out this process from a particle physics point of view. In Fig.6 we show the photon emission rates as a function of a suitably chosen Lorentz invariant, x, which basically measures the energy of the scattered photons in any chosen reference frame. The reference peak at the very right corresponds to standard (n=1) low intensity ($\alpha_0 \simeq 0$) Compton back scattering of laser photons colliding with a 40 MeV electron beam.

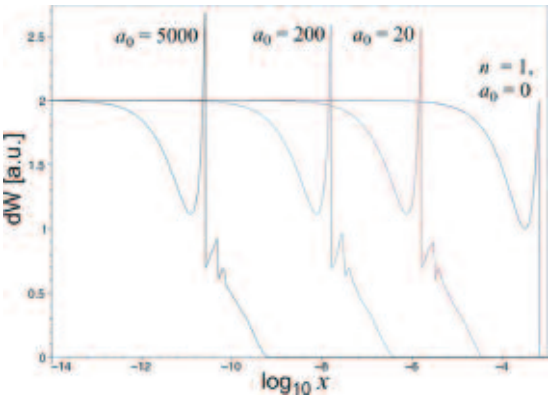

Figure 6. Photon emission rates for nonlinear Compton scattering and different values of a_0 as a function of the invariant x.

The most striking experimental signal is a red-shift of this linear Compton edge, from $4\gamma^2\hbar\omega_L$ to $4\gamma^2\hbar\omega_L/(1 + a_0^2)$. This may be understood in terms of the electron mass shift (12). As the electron 'gains weight' ($m \rightarrow m^*$) it will recoil less, reducing the energy transfer to the final state photon, hence the red-shift in the maximum photon energy. This effect is illustrated in the photon spectrum of Fig.6 for different a_0 values with a_0 = 200 being expected for the Vulcan 10 PW upgrade. For further intensity effects in Compton scattering the reader is referred to the recent synopsis [12].

Conclusions

We have given an overview of laser induced strong-field QED processes adopting the language of Feynman diagrams. Even the small segment of the whole 'zoo' of diagrams discussed here has already revealed a rich source of interesting physics. Certainly, a more systematic study is needed to include realistic beam shapes and further effects such as trident pair production, *bremsstrahlung* and variants thereof. The most important applications will presumably result from the generation of purposefully tailored beams, ranging from X-rays to electrons and even positrons.

Acknowledgements

I thank Chris Harvey and Anton Ilderton for a fruitful collaboration on strong-field QED and Kurt Langfeld for writing the programmes producing Figs 3 and 4.

References

1. T. Heinzl and A. Ilderton, *Opt. Commun*. **282**, 1879 (2009).
2. D. Volkov, *Z. Phys*. **94**, 250 (1935).
3. A. I. Nikishov and V. I. Ritus, Zh. Eksp. *Teor. Fiz*. **46**, 776, 1768 (1964); [*Sov. Phys. JETP* **19**, 529, 1191 (1964)].
4. W. Heisenberg and H. Euler, *Z. Phys*. **98**, 714 (1936).
5. J. S. Schwinger, On gauge invariance and vacuum polarization, *Phys. Rev*. **82**, 664 (1951).
6. F. Sauter, *Z. Phys*. **69**, 742 (1931).
7. N. B. Narozhny *et al*., *Phys. Lett A* **330**, 1 (2004).
8. J. Toll, PhD thesis, Princeton 1952 (unpublished).
9. T. Heinzl *et al*., *Opt. Commun*. **267**, 318 (2006).
10. C. Bamber *et al*., *Phys. Rev. D* **60**, 092004 (1999).
11. N. Sengupta, *Bull. Math. Soc*. (Calcutta) **41**, 187 (1949); **44**, 175 (1952); T. W. B. Kibble, *Phys. Rev*. **138**, B740 (1965).
12. C. Harvey, T. Heinzl and A. Ilderton, *Phys. Rev. A* **79**, 063407 (2009).